# Evidence for orbital ordering in LaCoO₃

G. Maris,[1] Y. Ren,[2] V. Volotchaev,[1] C. Zobel,[3] T. Lorenz,[3] and T. T. M. Palstra[1,*]

[1]*Solid State Chemistry Laboratory, Materials Science Centre, University of Groningen, Nijenborg 4, 9747 AG Groningen,*
*The Netherlands*
[2]*Argonne National Laboratory, 9700 South Cass Avenue, Argonne, Illinois 60439, USA*
[3]*II. Physikalisches Institut, Universität zu Köln, Zülpicher Strasse 77, 50937 Köln, Germany*

We present powder and single-crystal x-ray diffraction data as evidence for a monoclinic distortion in the low-spin ($S=0$) and intermediate spin states ($S=1$) of LaCoO₃. The alternation of short and long bonds in the *ab* plane indicates the presence of $e_g$ orbital ordering induced by a cooperative Jahn-Teller distortion. We observe an increase of the Jahn-Teller distortion with temperature in agreement with a thermally activated behavior of the $Co^{3+}$ ions from a low-spin ground state to an intermediate-spin excited state.

The study of orbital degrees of freedom in transition-metal (TM) oxides has gained prominent interest. Novel techniques such as resonant x-ray scattering and x-ray absorption spectroscopy (XAS) give direct information about orbital occupancy. It is realized that the orbital moments are as important as the spin moments to understand the electronic properties. Prominent examples in which the orbital degrees of freedom determine the electronic properties are the metal-insulator transitions in $V_2O_3$ (Ref. 1) and doped $LaMnO_3$.[2] Here, spin- and orbital-induced transitions are intimately related. In the perovskites, metallicity and orbital ordering are mutually exclusive because of the large Jahn-Teller (JT) splitting of the $e_g$ orbitals.[3] Furthermore, novel ground states can be obtained such as an orbital liquid.[4,5]

Considerable interest in the perovskite-type LaCoO₃ originates from the puzzling nature of two transitions in this compound and the vicinity to a metal-insulator transition. The ground state of LaCoO₃ is a nonmagnetic insulator and there is no long-range magnetic order at all temperatures. At low temperatures, the magnetic susceptibility increases exponentially with temperature exhibiting a maximum near 100 K. At higher temperatures, a second anomaly is observed around 500 K, which is accompanied by a semiconductor to metal transition. The maximum at 100 K was ascribed initially to a change of the spin state in the $Co^{3+}$ ions, i.e., a transition from a low-spin (LS) nonmagnetic ground state ($t_{2g}^6$, $S=0$) to a high-spin (HS) state ($t_{2g}^4 e_g^2$, $S=2$).[6–9] In the more recent literature,[10–14] new scenarios involving an intermediate-spin state (IS) ($t_{2g}^5 e_g^1$, $S=1$) have been proposed. Using LDA+U calculations, Korotin *et al.*[15] proposed the stabilization of the IS state due to the large hybridization between the Co-$e_g$ and O-2p levels. Due to the partially filled $e_g$ level, the IS state is JT active. The degeneracy of the $e_g$ orbitals of $Co^{3+}$ ions in the LS state is expected to be lifted in the IS state by a JT distortion.

All structural studies, based on powder x-ray and neutron-diffraction experiments are consistently interpreted in rhombohedral $R\bar{3}c$ symmetry and no structural transitions are reported in the temperature interval 4.2 K–1248 K.[16–19] A cooperative JT distortion is incompatible with this space group. The rhombohedral distortion of the parent cubic perovskite structure consists of a deformation along the body diagonal, and preserves only one Co—O distance. This triggered our present study to detect a coherent JT distortion and to investigate why recent high quality structural studies failed to observe such states. As the JT distortion caused by $e_g$ orbital ordering is usually quite large, there must be reasons why the distortion went unobserved. Furthermore, the LS-IS transition is robust and is observed both in powder and in single-crystal samples. A lattice distortion due to the JT effect in the IS state has been suggested by infrared spectroscopy measurements[13] and recently by magnetic susceptibility and thermal-expansion measurements.[20]

In certain cases it is exceedingly difficult to identify the correct crystal symmetry. In perovskites such as $LaMnO_3$ or $YVO_3$ the JT distortion involves alternating long and short TM-O distances without always lowering the symmetry of the lattice.[21] Consequently, refinement of powder-diffraction data are not very sensitive to several symmetry modifications and single-crystal diffraction is a prerequisite to determine the crystal symmetry. LaCoO₃ has been consistently analyzed with the rhombohedral space group $R\bar{3}c$. This rhombohedral symmetry involves an alternating rotation of the corner sharing CoO₆ octahedra along all three crystallographic axes of the undistorted, cubic perovskite parent structure. The corner sharing oxygen octahedra can be described by one oxygen position. This symmetry allows only one Co—O distance and thus rules out a coherent JT distortion. Such distortion, while preserving the alternating rotation of the CoO₆ octahedra, lowers the symmetry to monoclinic subgroups of $R\bar{3}c$. The monoclinic space group $I2/a$ (Refs. 22,23) a subgroup of $R\bar{3}c$ with the highest symmetry that accommodates the rotations of the octahedra as well as a coherent JT distortion. The symmetry reduction to $I2/a$ space group is caused by rotations of unequal magnitude and/or a differentiation of Co—O bond lengths, induced by a coherent JT distortion. In this symmetry two oxygen positions describe the oxygen framework. A shift of the second oxygen position with $x_{O_2} = y_{O_2}$ corresponds to a differentiation of Co—O bond lengths, whereas a movement perpendicular to this constraint results in a coherent rotation of the octahedra.

We provide strong evidence for such monoclinic distortion in the LS-IS state using high-resolution synchrotron single-crystal and powder-diffraction experiments. The monoclinic distortion is ascribed to a JT distortion that signals the long-range ordering of the $e_g$ orbitals. Our results are in agreement with the LS-IS state scenario in which the occupation of the IS states of the $Co^{3+}$ ions is thermally activated from the ground LS state.[20]

Single crystals of $LaCoO_3$ were grown by the floating-zone technique in an image furnace. High-resolution x-ray diffraction measurements were performed on a triple-axis high-energy diffractometer with a photon energy of 115 keV at the beamline 11ID-C, BESSRC CAT, Argonne National Laboratory. $\omega$-$\chi$ scans were collected on a single crystal of approximate dimension 1 mm. Full datasets were measured on a small single-crystal fragment of approximate dimension 0.1mm using Mo-$K_\alpha$ radiation. The measurements were collected using a Bruker SMART charge-coupled device camera and face indexed absorption corrections were performed using associated software packages.[24] The integration of the frames was carried out using the SAINT software[24] incorporating the absorption correction program SADABS. The separation of the twins was done using the GEMINI program.[24] Structural determination and refinement was carried out using the SHELXTL package.[24]

We measured the temperature dependence of the magnetization of single-crystal $LaCoO_3$. The magnetization can be fitted well with a nonmagnetic ground state ($t_{2g}^6$) and a thermally activated $S=1$ state ($t_{2g}^5 e_g^1$) with an activation energy of $\Delta \sim 180$ K, as shown recently by Zobel *et al.*[20] The stoichiometry of the crystal can be derived from the very small Curie-term, indicating less than 1% $S=1$ impurities. The impurity contribution gives rise to the deep minimum at 35 K in the magnetic susceptibility. The raising of this minimum in the powder samples is attributed to $Co^{2+}$ localized magnetic moments associated with the reconstruction of the surface.[9] The volume of this surface is larger for powder samples than for single crystals. Our single-crystal measurement shows a minimum susceptibility approximately two times smaller than in the powder samples.[12]

A full structure determination has been made by single-crystal x-ray diffraction. However, the crystals are highly twinned as is common both for orthorhombic and rhombohedral perovskites. Twinning can complicate the symmetry determination considerably.[25]

The rhombohedral perovskites are obtained by a compression of the parent cubic cell along one of the body diagonals. The twinning is a result of the four body diagonals of which only one unique axis is chosen. The twin law relates four twin fractions by 90° rotation about the cubic main axes. The diffraction pattern of our samples typically exhibited two or three rhombohedral twins. The twinning "masks" the reflection conditions associated with the lowering of the symmetry from $R\overline{3}c$ to $I2/a$, especially the $c$-glide plane and the threefold axis. First, the violation of the $c$-glide plane will give rise to extra reflections. However, these reflections are also generated by the rhombohedral twinning. Therefore, their presence cannot be used as evidence for monoclinic distor-
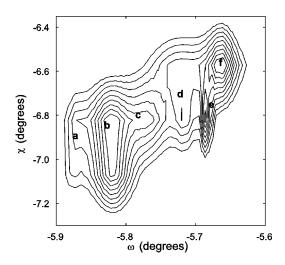


FIG. 1. The profile of a (10 2 8) reflection (Ref. 26) in an $\omega$-$\chi$ scan at 60 K. The two rhombohedral fractions positioned at $w_1 \sim -5.82°$ and $w_2 \sim -5.69°$ split further into three peaks representing the monoclinic twins and are labeled as a, b, c and d, e, f, respectively.

tion. Second, while the disappearance of the threefold symmetry does not generate new reflections, the resulting twinning mimics $R\overline{3}c$ symmetry. A small monoclinic distortion can give rise to such pseudomerohedral twinning, which can be easily overlooked in a standard analysis due to insufficient angular resolution. Therefore, high angular resolution single-crystal x-ray diffraction experiments are needed to determine the symmetry.

We verified the presence of twinning by performing $\omega$-$\chi$ scans with high angular resolution (0.01° per/step) using synchrotron radiation. Such scans measure a cross section of reciprocal space on the Ewald sphere perpendicular to the scattering vector. In this way we measure the fine structure of a Bragg peak caused by twinning. Figure 1 shows such a profile of a (10 2 8) reflection[26] in an $\omega$-$\chi$ scan measured at 60 K. The two big spots that split by 0.15(1)° in $\omega$, correspond to two twins generated by lowering the symmetry from cubic to rhombohedral. Each of these rhombohedral twins shows a further splitting of about 0.04(1)° in $\omega$. This smaller splitting is best observed at 20 K and 60 K, but also the measured rhombohedral peaks at 120 K and room temperature show clear shoulders. We attribute this smaller splitting to the twinning caused by the decrease in symmetry from rhombohedral to monoclinic. The same type of profiles are observed for all the peaks we have measured on several crystals. Such splitting indicates a distortion from the rhombohedral unit-cell parameters. The observed splitting indicates that the monoclinic symmetry is maintained in the temperature interval 20 K–300 K.

After establishing the symmetry of the structure, the atomic positions can be determined from standard single-crystal diffraction experiments. Full datasets were measured at different temperatures (90 K, 120 K, 140 K, 160 K, 200 K, 250 K, and 295 K) on a Bruker APEX diffractometer, using Mo-$K_\alpha$ radiation. The rhombohedral twinning was clearly observable and the twins were analyzed separately. However, the monoclinic twinning could not be observed on this dif-

TABLE I. Lattice parameters for LaCoO$_3$.

| $T$ | $a$ | $b$ | $c$ | $\beta$ | Volume |
|---|---|---|---|---|---|
| 295 | 5.3695(4) | 5.4331(4) | 7.6395(6) | 90.985(5) | 222.83(4) |
| 250 | 5.3672(4) | 5.4329(4) | 7.6367(5) | 91.014(4) | 222.65(4) |
| 200 | 5.3611(3) | 5.4316(3) | 7.6318(4) | 91.056(3) | 222.20(3) |
| 160 | 5.3578(2) | 5.4291(2) | 7.6288(3) | 91.108(3) | 221.86(2) |
| 140 | 5.3585(2) | 5.4316(2) | 7.6304(3) | 91.126(2) | 222.04(2) |
| 120 | 5.3544(2) | 5.4294(2) | 7.6257(2) | 91.148(2) | 221.64(2) |
| 90 | 5.3469(3) | 5.4227(3) | 7.6168(4) | 91.174(3) | 220.80(2) |

TABLE III. Selected bond distances in angstron for LaCoO$_3$.

| Temp (K) | Co-O$_2$ (Å) | Co-O$_1$ (Å) | Co-O$_2$ (Å) |
|---|---|---|---|
| 295 | 1.874(7) | 1.925(8) | 1.993(8) |
| 250 | 1.877(6) | 1.9357(9) | 1.9792(6) |
| 200 | 1.892(7) | 1.9326(9) | 1.962(7) |
| 160 | 1.889(6) | 1.9329(9) | 1.962(6) |
| 140 | 1.882(6) | 1.9332(9) | 1.972(6) |
| 120 | 1.879(6) | 1.9325(9) | 1.971(5) |
| 90 | 1.918(6) | 1.9235(8) | 1.934(6) |

fractometer due to insufficient angular resolution. The presence of the monoclinic twins was observed on a Enraf-Nonius CAD4 diffractometer equipped with a point detector, which yields a better angular resolution. Again, these measurements indicate the splitting of the rhombohedral peaks as evidence for monoclinic distortion. However, for structural refinement, the monoclinic twin fractions could not be separated. Therefore, the unit-cell parameters derived from the single-crystal measurements are averaged at their rhombohedral values (Table I). The intensities of the reflections were obtained from the largest rhombohedral twin fraction, which includes the integrated intensity of the monoclinic twin fractions together. Nevertheless, precise positions of the atoms can be obtained by making use of the monoclinic twin relation in the refinements.

The pseudomerohedral twinning in LaCoO$_3$ results from the loss of threefold symmetry during the crystal growth or a structural phase transition at elevated temperature. Therefore, the twinning corresponds to the three possibilities of converting the rhombohedral axes in $R\bar{3}c$ symmetry into the $c$ axis in monoclinic symmetry. There is no physical reason for one twin to be favored over the others and equal volume fractions can be expected. All crystals that we investigated exhibited such a monoclinic twinning. The twin law relates three twin fractions by 120° rotation about the cubic [111] direction. If the twin fractions are equal, the reflections $(h,k,l)$ (Ref. 26) and cyclic permutations have equal intensities and simulate the existence of a threefold axis. Thus, it is not surprising that the quality of the refinements in both $R\bar{3}c$ and $I2/a$ space groups is essentially the same. However, by introducing this twin model, the quality of the refinements in $I2/a$ space group was improved, the resulting $R1$ values falling for a typical dataset (140 K) from 0.0445 to 0.0433. The refined values of the twin fractions range between 30% and 40%. The atomic coordinates for a typical dataset (200 K) and the selected bond lengths are displayed in Tables II and III, respectively.

TABLE II. Atomic parameters for LaCoO$_3$ at 200 K.

| Atom | Position | x | y | z | $U_{iso}$ |
|---|---|---|---|---|---|
| La | 4e | 0.25 | 0.25019(13) | 0 | 0.00486(11) |
| Co | 4c | 0.75 | 0.25 | 0.25 | 0.00452(13) |
| O1 | 4e | 0.25 | −0.3068 | 0 | 0.0101(15) |
| O2 | 8f | 0.0241(10) | 0.0332(10) | 0.2293(7) | 0.0044(6) |

Recent high-resolution powder neutron-diffraction measurements were analyzed with $R\bar{3}c$ symmetry and failed to identify a monoclinic distortion.[18] We performed experiments on high quality powder obtained from a crushed single crystal using synchrotron radiation and high angular resolution: 0.001° per step. We measured the temperature dependence of the profile of the (4 0 0) reflection[26] as the degeneracy of this peak is expected to be lifted by lowering the symmetry from rhombohedral $R\bar{3}c$ space group to monoclinic $I2/a$ space group. The peak width is resolution limited (0.0025°) up to 65 K and it starts to broaden gradually as the temperature is increased, reaching 0.0036° at 145 K. We associate the broadening of the Bragg reflection with a gradual distortion of the structure. The monoclinic symmetry is compatible with a splitting of this reflection. In the left side of Fig. 2 we show the temperature dependence of the splitting of the (4 0 0) reflection derived from the peak profiles. In the inset of Fig. 2 we show the profiles of the peak at 45 K and 120 K. The splitting in $\omega$ derived from the $\omega$-$\chi$ scans on single crystals corresponds to a much smaller splitting in $\theta$-$2\theta$ scans in the Bragg geometry. Thus, due to limitation in angular resolution, the monoclinic distortion can go easily undetected in Bragg geometry powder x-ray diffraction.
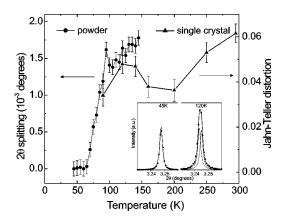


FIG. 2. Left: Temperature dependence of the splitting of (4 0 0) reflection (Ref. 26) in $\theta$-$2\theta$ geometry (below 65 K the linewidth is resolution limited). Right: The JT distortion parameter versus temperature as determined from the single-crystal refinements. The lines are guides for the eye. Inset: Profile of (4 0 0) reflection at 45 K and 120 K. The profile at 120 K can be accurately fitted by two Lorentzians with the linewidth of the 45 K data.

We notice that powder and single-crystal diffraction give complementary information. The single-crystal analysis is of crucial importance for detecting the lowering of the symmetry. However, analyzing the single-crystal data turns to be difficult due to pseudomerohedral twinning and only yields proper crystallographic results when appropriate symmetry and twinning are used. No accurate lattice parameters can be derived from single-crystal x-ray diffraction as they are averaged by the twinning. Nevertheless, the rotation and JT distortion can be accurately determined from a refinement. Once the correct space group is assigned, the lattice parameters can be more precisely determined from a powder x-ray diffraction measurement.

We derive three unequal Co—O bond lengths over the studied temperature range: one short, one long, and one medium. The long and short Co–O distances correspond to the bonds in the $ab$ plane, while the medium Co—O distances are the out-of-plane bonds. These results indicate a clear coherent Jahn-Teller effect associated with a $Q2$ type of distortion.[27] The right side of Fig. 2 shows the temperature dependence of the Jahn-Teller parameter, defined as the difference between the long and short bond lengths normalized by their average. The magnitude of the JT parameter increases with temperature, reaching $\sim 6\%$ at room temperature. This value is somewhat smaller than the JT distortion of $\sim 10\%$ found in LaMnO$_3$ at room temperature.[28]

The distortion of the octahedra lifts the degeneracy of the $e_g$ orbitals and XAS data[29] show that the $z^2$-like orbitals are thermally populated. The $z^2$-like orbitals have an antiferrodistortive ordering along all three directions suggesting a ferromagnetic coupling between magnetic sites.[15] Such a ferromagnetic exchange interaction is also supported by polarized neutron measurements.[6] An antiferrodistortive orbital ordering giving rise to ferromagnetic interactions was also found in YTiO$_3$, where the $t_{2g}$ orbitals of Ti$^{3+}$ cations are occupied by a single electron.[30] However, for this system the JT distortion involves $t_{2g}$ orbitals for which the magnitude of the distortion is roughly five times smaller than for $e_g$-based JT systems.

The discovery of a coherent JT distortion in LaCoO$_3$ offers deeper insight and is unexpected considering the scrutiny with which this compound was studied. It is clear that the JT distortion may have gone unnoticed in single-crystal x-ray diffraction experiments because of twinning. Moreover, the JT distortion is not easily detected by powder x-ray diffraction because of the very small monoclinic distortion.

Our measurements are in agreement with the recent magnetic and XAS measurements,[20,29] which were interpreted with a thermal activation of the IS spin state. Considering the fact that LaCoO$_3$ is close to a metallic ground state, the transition may involve more complex behavior. It is observed in the manganites[3,31] that phase coexistence of metallic and insulating states arises from a competition between JT-distorted and non-JT distorted regions in the sample. The propagation of strain in the crystal may result in an appearance that closely resembles a transition. Such phase coexistence requires detailed real space measurements.

We conclude that LaCoO$_3$ exhibits a monoclinic distorted structure in the temperature interval 20–300 K. The monoclinic distortion state is brought about by a cooperative Jahn-Teller effect that triggers the long-range orbital ordering of the $e_g$ orbitals. The gradual increasing with temperature of the Jahn-Teller distortion suggests the thermal population of the IS state of the Co$^{3+}$ ions.

*Corresponding author. Email address: palstra@chem.rug.nl

[1] L. Paolasini, C. Vettier, F. dc Bergevin, F. Yakhou, D. Mannix, A. Stumault, W. Neubeck, M. Altarelli, M. Fabrizio, P.A. Metcalf, and J.M. Honig, Phys. Rev. Lett. **82**, 4719 (1999).

[2] Y. Murakami, J.P. Hill, D. Gibbs, M. Blume, I. Koyama, M. Tanaka, H. Kawata, T. Arima, Y. Tokura, K. Hirota, and Y. Endoh, Phys. Rev. Lett. **81**, 582 (1998).

[3] B.B. Van Aken, O.D. Jurchescu, A. Meetsma, Y. Tomioka, Y. Tokura, T.T.M. Palstra, Phys. Rev. Lett. **90**, 066403 (2003).

[4] G. Khaliullin and S. Maekawa, Phys. Rev. Lett. **85**, 3950 (2001).

[5] B. Keimer, D. Casa, A. Ivanov, J.W. Lynn, M.v. Zimmermann, J.P. Hill, D. Gibbs, Y. Taguchi, and Y. Tokura, Phys. Rev. Lett. **85**, 3946 (2000).

[6] K. Asai, O. Yokokura, and N. Nishimori, Phys. Rev. B **50**, 3025 (1994).

[7] M. Itoh, I. Natori, S. Kubota, and K. Motoya, J. Phys. Soc. Jpn. **63**, 1486 (1994).

[8] S. Yamaguchi, Y. Okimoto, H. Taniguchi, and Y. Tokura, Phys. Rev. B **53**, 2926 (1996).

[9] M.A. Señaris Rodríguez and J.B. Goodenough, J. Solid State Chem. **116**, 224 (1995).

[10] R.H. Potze, G.A. Sawatzky, and M. Abbate, Phys. Rev. B **51**, 11 501 (1995).

[11] T. Saitoh, T. Mizokawa, A. Fujimori, M. Abbate, Y. Takeda, and M. Takauo, Phys. Rev. B **55**, 4257 (1997).

[12] K. Asai, A. Yoneda, O. Yokokura, J.M. Tranquada, G. Shirane, and K. Kohn, J. Phys. Soc. Jpn. **67**, 290 (1998).

[13] S. Yamaguchi, Y. Okimoto, and Y. Tokura, Phys. Rev. B **55**, 8666 (1997).

[14] Y. Kobayashi, N. Fujiwara, S. Murata, K. Asai, and H. Yasuska, Phys. Rev. B **62**, 410 (2000).

[15] M.A. Korotin, S.Yu. Ezhov, I.V. Solovyev, and V.I. Anisimov, Phys. Rev. B **54**, 5309 (1996).

[16] Y. Kobayashi, T. Mitsunaga, G. Fujinawa, T. Arii, M. Suetake, K. Asai, and J. Harada, J. Phys. Soc. Jpn **69**, 3468 (2000).

[17] G. Thornton, B.C. Tofield, and A.W. Hewat, J. Solid State Chem. **61**, 301 (1986).

[18] P.G. Radaelli and S-W. Cheong, Phys. Rev. B **66**, 094408 (2002).

[19] D. Louca, J.L. Samo, J.D. Thompson, H. Rodes, and G.H. Kari, Phys. Rev. B **60**, 10 378 (1999).

[20] C. Zobel, M. Kriener, D. Bruns, J. Baier, M. Grüninger, and T. Lorenz, Phys. Rev. B **66**, 020402(R) (2002).

[21] G.R. Blake, T.T.M. Palstra, Y. Ren, A.A. Nugroho, and A.A. Menovsky, Phys. Rev. Lett. **87**, 245501 (2001).

[22] The unit cell of $a \approx 9.26$ Å, $b \approx 5.43$ Å, $c \approx 5.37$ Å, $\beta \approx 124.4°$ in the standard setting $C2/c$ is transformed to $a \approx 5.37$ Å, $b \approx 5.43$ Å, $c \approx 7.64$ Å, $\beta \approx 91°$ in $I2/a$ setting.

[23] A.M. Glazer, Acta Crystallogr., Sect. A: Cryst. Phys., Diffr., Theor. Gen. Crystallogr. **A31**, 756 (1975).

[24] G.M. Sheldrick, *SAINT+NT*, *Version 6.02a*, *GEMINI, SHELXTL, TOPAS 2.0* (Brucker Analytical X-ray instruments Inc., Madison, WI, USA).

[25] B.B. Van Aken, A. Meetsma, Y. Tomioka, Y. Tokura, and T.T.M. Palstra, Phys. Rev. B **66**, 224414 (2002).

[26] The Miller indices refer to the double cubic unit cell.

[27] J. Kanamori, J. Appl. Phys. **31**, 14S (1960).

[28] J. Rodríguez-Carvajal, M. Hennion, F. Moussa, and A.H. Moudden, Phys. Rev. B **57**, R3189 (1997).

[29] Z. Hu and L. H. Tjeng (private communications).

[30] H. Sawada and K. Terakura, Phys. Rev. B **58**, 6831 (1998).

[31] N. Mathur and P. Littlewood, Phys. Today **56** (1), 25 (2003).